

ROTATION AND X-RAY EMISSION FROM PROTOSTARS

THIERRY MONTMERLE¹ AND NICOLAS GROSSO

Service d'Astrophysique, CEA/DAPNIA/Sap, Centre d'Etudes de Saclay, 91191 Gif-sur-Yvette Cedex, France

YOHKO TSUBOI

Department of Astronomy & Astrophysics, Penn State University, University Park, PA 16802, USA

AND

KATSUJI KOYAMA²

Department of Physics, Faculty of Science, Kyoto University, Sakyo-ku, Kyoto 606-8502, Japan

Received 1999 July 12; accepted 1999 November 18

ABSTRACT

The ASCA satellite has recently detected variable hard X-ray emission from two Class I protostars in the ρ Oph cloud, YLW15 (IRS43) and WL6, with a characteristic time scale ~ 20 h. In YLW15, the X-ray emission is in the form of quasi-periodic energetic flares, which we explain in terms of strong magnetic shearing and reconnection between the central star and the accretion disk. The flare modelling, based on the solar analogy, gives us access to the size of the magnetic structures, which in turn allows to calculate the rotation parameters of the star and the disk. In WL6, X-ray flaring is rotationally modulated, and appears to be more like the solar-type magnetic activity ubiquitous on T Tauri stars. On the basis of these observations, we find that YLW15 is a fast rotator (near break-up), while WL6 rotates with a significantly longer period. We thus use X-ray flaring as a “clock” to measure the rotation of protostars. With the help of the mass-radius relation on the stellar “birthline”, we derive a mass $M_\star \sim 2M_\odot$ and $\lesssim 0.4M_\odot$ for the central stars of YLW15 and WL6 respectively. YLW15 thus appears as a future A star. On the long term, the magnetic interactions between the star and the disk results in magnetic braking and angular momentum loss of the star. The compared rotation behavior of YLW15 and WL6 confirms that for solar-mass stars their magnetic braking takes place on time scales $t_{br} \sim$ a few 10^5 yrs, i.e., of the same order as the estimated duration of the Class I protostar stage. The main parameter determining t_{br} turns out to be the stellar mass, so that close to the birthline there must be a mass-rotation relation, $t_{br} \propto M_\star$, such that stars with $M_\star \gtrsim 1 - 2M_\odot$ are fast rotators, while their lower-mass counterparts have had the time to spin down and reach synchronous rotation with the inner surrounding accretion disk. The rapid rotation and strong star-disk magnetic interactions of YLW15 also naturally explain the observation of “superflares” of X-ray luminosities as high as $L_X \gtrsim 10^{33-34}$ erg s⁻¹ during a few hours, while at the WL6 stage the lower X-ray luminosities are likely to be of purely stellar origin. The mass-rotation relation through magnetic braking may also explain why so few Class I protostars have been detected in X-rays to date, and why they all lie in clusters. In the case of YLW15, and perhaps also of other protostars, a hot coronal wind ($T \sim 10^6$ K) may be responsible for the VLA thermal radio emission. This paper thus proposes the first clues to the magnetic properties of protostars, which govern their rotation status and evolution.

Subject headings: X-rays: stars – stars: rotation – stars: pre-main sequence – stars: individual (YLW15, WL6) – stars: flare – stars: magnetic fields – stars: mass loss

1. INTRODUCTION

Using the ASCA satellite, Tsuboi et al. (1999; hereafter Paper I) have recently detected approximately periodic (characteristic time scale ~ 20 h) X-ray emission from one remarkable protostar in the nearby ($d \sim 160$ pc)³ ρ Ophiuchi cloud core region, YLW15 (Young, Lada, & Wilking 1986), also known as IRS43 (Wilking, Lada, & Young 1989), at a level of $L_X = 20 - 5 \times 10^{31}$ erg s⁻¹. This protostar belongs to the so-called “Class I” stage, characterized by a strong mid-IR excess, and corresponds to the final phases of the accretion process, where most of the mass is contained in the central star,

with comparatively little left in the circumstellar envelope. The infalling material transits mostly via an accretion disk (e.g., André & Montmerle 1994: AM; André, Ward-Thompson & Barsony 2000: AWB). YLW15 displayed quasi-periodic X-ray flares; prior to this observation, YLW15 was seen by the ROSAT High Resolution Imager (HRI) to emit a “superflare” with a peak X-ray luminosity $L_X \gtrsim 10^{33-34}$ erg s⁻¹ during a few hours (Grosso et al. 1997).

The main properties of YLW15 can be summarized as follows. Its bolometric luminosity is $L_{bol} \sim 10L_\odot$ (Wilking, Lada & Young 1989), making it one of the most luminous protostars in the ρ Oph Core F region. It is surrounded by

¹Send offprint request to montmerle@cea.fr.

²CREST, Japan Science and Technology Corporation (JST), 4-1-8 Honmachi, Kawaguchi, Saitama, 332-0012, Japan

³The 165 pc value from Dame et al. 1987 was adopted in paper I to estimate the intrinsic X-ray luminosities.

a relatively dense, compact dusty envelope with outer radius $R_{out} \lesssim 3000$ AU, and total (gas + dust) mass $M_{env} = 0.05\text{--}0.3 M_{\odot}$ (AM; Motte, André, & Neri 1998; MAN). The slope of its infrared (IR) spectral energy distribution (SED), $\alpha_{IR} = d(\log \lambda F_{\lambda})/d\log \lambda = 1.2$, led to its early classification as a Class I protostar. From *JHK*L photometry, one can compute the extinction, which suffers a large uncertainty: $A_{V,IR} \sim 20\text{--}40$, with a “preferred” value $A_{V,IR} \sim 30$, or equivalently $N_H \sim 6.7 \times 10^{22} \text{ cm}^{-3}$ (see discussion in Grosso et al. 1997). The X-ray spectral fitting yields $A_{V,X} \sim 15$ (Paper I), which can be considered as an acceptable agreement considering the rather large uncertainties on $A_{V,IR}$; alternatively, this difference could be due to a smaller gas-to-dust ratio in dense molecular cores. YLW15 also powers a compact bipolar CO outflow (Bontemps et al. 1996), and exhibits a circumstellar disk $\gtrsim 500$ AU in radius, seen approximately edge-on in *HST* – *NICMOS* images (Terebey et al. 1999, in preparation). In addition, with a VLA 6-cm flux density of 3.3 mJy, it is by far the brightest stellar radio continuum source of Core F (Leous et al. 1991), which is likely of thermal origin (André et al. 1992). YLW15 is thus confirmed to be a bona-fide Class I protostar, at an intermediate stage of evolution between the younger “Class 0” protostars (André, Ward-Thompson, & Barsony 1993, AWB) and “flat-spectrum” protostars (AM). The estimated age of such protostars is $\sim 0.75\text{--}1.5 \times 10^5$ yr (Luhman & Rieke 1999).

In this paper, we argue that the quasi-periodic X-ray flares of YLW15 can be explained by fast rotation of the central star with respect to the inner accretion disk, which results in star-disk shearing of the magnetic field lines, producing magnetic reconnection and mass loss, and eventually extremely high X-ray luminosities. On the other hand, we show that magnetic braking, due to the coupling between the star and the disk, occurs on timescales typically \lesssim a few 10^5 yrs, i.e., on the order of the age of Class I protostars. This braking asymptotically leads to synchronous rotation between the central star and the inner accretion disk (period \sim a few days). Comparing the X-ray light curves of YLW15 and of WL6, another Class I protostar in the ρ Oph core F showing rotational modulation in X-rays corresponding to a period ~ 3 days, we argue that, in contrast to YLW15, WL6 should have essentially reached a slow rotation stage, with “classical” T Tauri (Class II) X-ray properties.

The outline of the paper is as follows. We first concentrate on YLW15, studying the implications of the quasi-periodic flares seen by ASCA (§2) in terms of fast rotation of the central star: we first establish the connection between the flare periodicity and the rotation parameters of the star and the accretion disk (§2.1), then we study the long-term implications for the magnetic braking of protostars (§2.2) and for their angular momentum loss (§2.3); finally we point out some consequences on the X-ray flare energetics (§2.4). We then turn to WL6, reexamining its light curve to conclude that it is a slow rotator (§3), and we derive the stellar parameters for YLW15 and WL6 (§4). From the comparison of the properties of these two Class I protostars, we examine briefly in §5 the consequences of the fast rotation of protostars on the magnetic braking time scale as a function of the stellar mass, and on the accretion process; we also propose an explanation of the fact that few Class I protostars have been detected in X-rays so far, all in clusters; and finally we discuss the main areas of uncertainty affecting these conclusions. In the last section (§6), we summarize the paper and conclude by a short synthesis of the possible history of rotation and magnetic activity of protostars.

2. IMPLICATION OF THE QUASI-PERIODIC FLARES OF YLW15

2.1. The rotation connection

2.1.1. X-ray periodicity observations of YLW15

The ASCA observations of YLW15 analyzed in Paper I show well-characterized flaring with an approximate period $P_f \equiv 2\pi/\Omega_f \sim 20$ hrs. Fig. 1 shows the X-ray light curve of YLW15 in the 2–10 keV domain. At least the first flare can be well-modeled by the quasi-static radiative cooling of a semi-circular magnetic loop-shaped tube (Van den Oord & Mewe 1989) of length $\sim 14 R_{\odot}$, i.e. $\sim 4.5 R_{\odot}$ in radius, and aspect ratio $a = (\text{cross-section diameter})/(\text{loop length}) \simeq 0.07$. The e-folding decay time of the flare is ~ 30 ksec, i.e., less than half of the flare period. The peak luminosities are $L_{X,peak} \sim 2 \times 10^{32} \text{ erg s}^{-1}$ for the first flare, and $\approx 8\text{--}5 \times 10^{31} \text{ erg s}^{-1}$ for the other two flares; the total energies released are respectively $E_{tot} \sim 6.5 \times 10^{36} \text{ erg}$ for the first flare, and $\approx 3 \times 10^{36} \text{ erg}$ for the second and third flare. The values derived in Paper I for the plasma density ($n_e \sim 5 \times 10^{10} \text{ cm}^{-3}$) and the equipartition magnetic field of each flare ($B_{eq} \sim 100\text{--}150$ G) are comparable to those of solar coronal plasmas, which justifies here again, as in all YSOs, the use of the solar analogy as a basis to analyze the implications of the triple flare of YLW15. (For reference, see the review by Feigelson & Montmerle 1999: FM.)

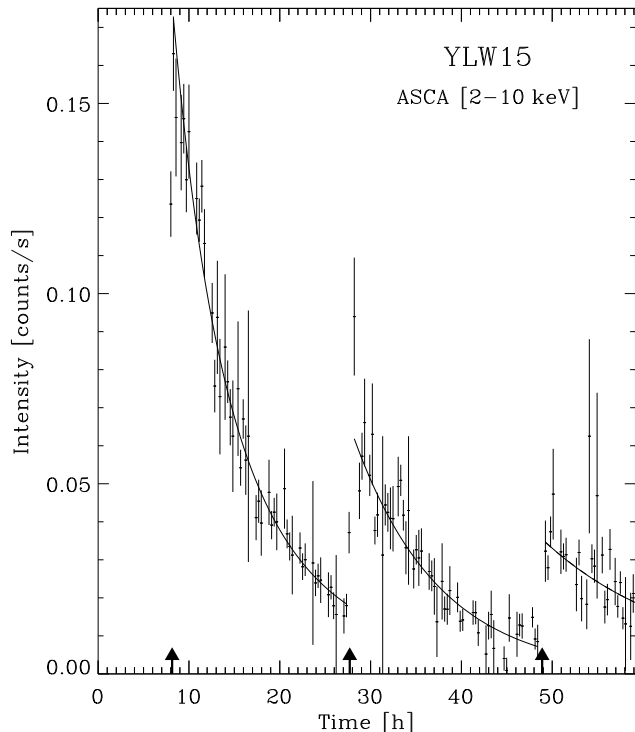


Fig. 1.— Light curve of YLW15 obtained with ASCA (Tsuboi et al. 1999: Paper I). The data points of the first flare are fitted with a quasi-static radiative cooling model, and those of the other two flares are fitted by exponentials with radiative cooling timescales (see Paper I for details). The arrows point at the start of the flares, with a characteristic interval ~ 20 h.

Now the ASCA observation of Paper I could be considered as a random event. However, there is some evidence that the same ~ 20 h period was already present in *Tenma* observations over a decade ago (Koyama 1987). *Tenma* was a wide-field, non-imaging satellite, sensitive to hard X-rays like ASCA. The observation covered the whole ρ Oph cloud.

The derived temperature ($kT \sim 4$ keV) and X-ray luminosity ($L_X[1.5 - 10 \text{ keV}] \sim 1.8 \times 10^{32} \text{ erg s}^{-1}$) are comparable with those of the triple flare observed with ASCA ($kT \sim 2 - 6$ keV, and $L_X[2 - 10 \text{ keV}] \sim 11 - 2 \times 10^{31} \text{ erg s}^{-1}$). These properties were from the start puzzlingly different from those derived from *Einstein* images of the same region, which showed only T Tauri stars with $kT \sim 1$ keV and $L_X(0.5 - 4.5 \text{ keV}) \sim 2 - 20 \times 10^{30} \text{ erg s}^{-1}$ (Montmerle et al. 1983). Nowadays, it is well known from ASCA images showing both protostars and T Tauri stars in the field-of-view that protostars are preferentially detected in the hard X-ray band (\gtrsim a few keV), in contrast with the dominant population of T Tauri stars, which generally emit softer X-rays and are less luminous (e.g., Fig. 1 of Paper I, and Figs. 1a and 1b of Koyama et al. 1996). In retrospect, this *Tenma* result is therefore totally consistent with the interpretation that YLW15 dominated the X-ray flux of all YSOs in the field-of-view at the time of the observation.

This suggests that the characteristic timescale of ~ 20 h is a long-lived feature, directly related to an intrinsic property of YLW15, and not related to flare events *a priori* randomly distributed in time. The simplest explanation is that *the X-ray flare period must be closely related to the stellar rotation period*.

2.1.2. Star-disk magnetic interactions

The analysis of the X-ray properties of the YLW15 triple flare presented in Paper I indicates that we are certainly in the framework of magnetically induced X-ray activity classically invoked for this type of object (see, e.g., FM). However, the X-ray periodicity underlying the flares is a novel feature which cannot be easily explained in terms of stellar activity alone. Given the existence of a previously observed X-ray “superflare” on the same object, with the unavoidable necessity of invoking some form of star-disk magnetic interaction as a corollary (Grosso et al. 1997), we also adopt this framework to interpret the origin of the triple flare.

Calculations of magnetic configurations resulting from star-disk magnetic shearing have recently been performed in the context of the origin of jets and outflows from young stellar objects (YSOs). These calculations have shown that an initially poloidal field line, anchored both in the star and in the disk, is twisted and inflated when the footpoints are not rotating synchronously. As a result, an increasingly large toroidal component develops (see, e.g. the helical configuration of Lovelace, Romanova, & Bisnovaty-Kogan 1995). This configuration allows antiparallel segments of the field lines to be brought in contact and give rise to reconnection. Theoretically, this reconnection can take place within the same field line, as in the solar case (giving rise to the “helmet” configuration, e.g., Hayashi, Shibata, & Matsumoto 1996), or between different field lines, as may happen for accreting neutron stars (Aly & Kuijpers 1990). So far, the field topology has been calculated only in 2D and 2.5D (see the numerical simulations by Hayashi, Shibata, & Matsumoto 1996; Goodson, Winglee, & Boehm 1997; Hirose et al. 1997; Miller & Stone 1998), and in 3D assuming axisymmetry (Fendt & Elstner 1999), but the Sun gives many observational examples of distorted topologies giving rise to reconnection (e.g., Innes et al. 1997). Additional mechanisms include resistive tearing instabilities in YSO magnetosphere-disk interactions (Birk 1998), and, as was studied numerically in the solar case by Amari et al. (1996), the twisting of a magnetic tube rooted in counter-rotating convective cells in the photo-

sphere. Obviously, there is no shortage of possible reconnection scenarios.

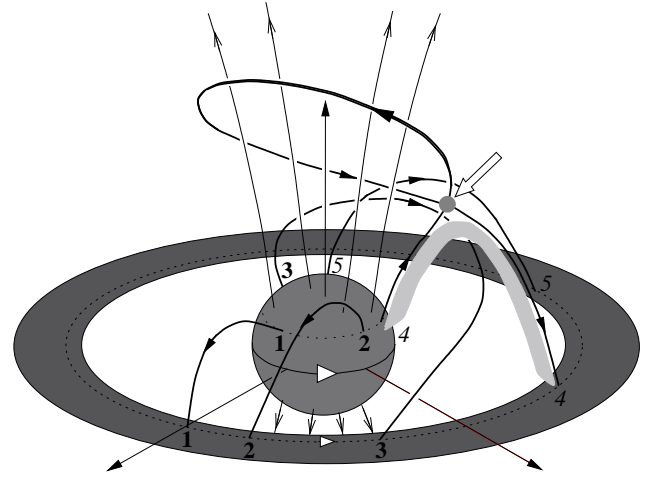


Fig. 2.— Sketch of the plausible evolution of a magnetic field configuration leading to reconnection and flaring for the quasi-periodic light curve of YLW15. This is just one of the possible configurations (see text, §2.1.2 for discussion). The open lines are other, unperturbed field lines. This figure schematically describes five steps of the evolution of a field line assumed to initially connect the star of period P_* and the inner disk of period P_{disk} (step 1). For illustrative purposes, we have chosen $P_* = P_{\text{disk}}/4$, thus $P_{\text{beat}} \equiv |1/P_* - 1/P_{\text{disk}}|^{-1} = 4P_*/3$: at steps 4 and 5 (in italics), the star has rotated more than one period. Since the star rotates faster than the inner disk, at steps 2 and 3 the magnetic field is sheared between the star and the disk, and the loop progressively inflates and surrounds ordered open stellar magnetic field lines. At step 4, the stellar footpoint has moved one beat period, so the initial field line comes into contact with itself (open arrow) and reconnects. The magnetic energy thus liberated heats the plasma and ignites a flare. (The shaded loop-like “brush stroke” schematically underlines the loop remaining after reconnection derived in Paper I, which we use for calculations in the present paper.) Step 5 illustrates the post-reconnection configuration, in which the plasma is radiatively cooling by X-ray bremsstrahlung and line emission. The scenario can then repeat itself if the magnetic field of step 4 reverts to the initial configuration after the reconnection (after step 5); in that case, successive reconnections and flaring may continue periodically for some time.

Fig. 2 illustrates one plausible scenario for the evolution of the configuration of magnetic field lines connecting the star and the accretion disk. Such an evolution leads to growth of the magnetic energy stored in the field lines at the expense of the star-disk mechanical energy, followed by local reconnection resulting in fast heating of the plasma and flaring. The figure schematically describes five steps of the evolution of a field line (or more realistically, as we have seen in Paper I, a thin tube) assumed to initially be anchored in the star and in the disk. The caption gives some details for each step. In brief, since the star rotates faster than the disk (this is demonstrated below), the magnetic field is sheared between the star and the disk, and the trailing loop progressively inflates and surrounds ordered open stellar magnetic field lines. The magnetic energy liberated when reconnection occurs heats the plasma and ignites a flare. The scenario can then repeat itself if the anchored part of the magnetic field reverts to the initial configuration after the reconnection; in that case, successive reconnections and flaring may continue periodically, at least for some time.

We have chosen this type of scenario because of the fact that in the quasi-periodic flares of YLW15 observed by ASCA, the

radii of the plasma confining loops do not change much in the three successive flares ($R_{loop} \sim 4.5R_\odot$), and radiative cooling models give good fits to their light curves. As discussed in detail in Paper I, these observations are consistent with the conclusion that *some basic magnetic structure, approximated by a semi-circular loop, has been reconstituted three times after reconnection, in a periodic fashion*. This is schematically illustrated in Fig. 2 in the form of a shaded loop-like “brush stroke”.

2.1.3. Determination of the star and disk rotation parameters

Taking this interpretation as a starting point, we are now in a position to derive the rotation parameters of the star and the disk in three steps: (i) investigate the relative kinematics of the star and the inner disk, where the loop footpoints are assumed to be anchored, (ii) use solar plasma physics to set constraints on star-disk magnetic field shearing and flare ignition, and (iii) combine the results.

Let A and B be the magnetic footpoints separated by a distance $2R_{loop}$, respectively located on the star (radius R_*) and the disk (radius $r_D \approx R_* + 2R_{loop}$): A rotates at some unknown stellar period P_* , and the Keplerian rotation period of the disk at B is $P_D \equiv 2\pi/\Omega_D$. We here adopt the view that the field lines and matter are strongly coupled: this is justified by the fact that a high ionization rate must be present in the disk, precisely because of X-ray irradiation (see Glassgold, Najita, & Igea 1997). In our scenario, the observed flare period P_f is therefore some fraction α of the (*a priori* unknown) beat period P_{beat} between A and B :

$$P_f = \alpha P_{beat} \quad (1)$$

with

$$1/P_{beat} \equiv |1/P_D \pm 1/P_*|. \quad (2)$$

Adopting the natural hypothesis that the star and the disk rotate in the same direction, and expressed in terms of positive periods, this equation can be rewritten as:

$$P_* = \begin{cases} 1/(1/P_D + 1/P_{beat}) & \text{if } P_* \leq P_D, \\ 1/(1/P_D - 1/P_{beat}) & \text{if } P_* \geq P_D. \end{cases} \quad (3)$$

In our case, for a given stellar mass and radius, P_D is a function of the star-disk distance r_D , itself ultimately fixed by the flaring loop size. Figure 3 schematically shows P_* as a function of P_D (Eq. 3) in the form of two half hyperbolae, with asymptotes at $P_* = P_{beat}$ and $P_D = P_{beat}$. For $P_D < P_{beat}$, there are two solutions, above and below the $P_* = P_D$ bisector: one corresponds to $P_* < P_D$ (the star rotates faster than the disk), the other to $P_* > P_D$ (the disk rotates faster than the star).⁴ For $P_D > P_{beat}$, there is only one solution, with $P_* < P_D$. These solutions may be interpreted as follows: for small values of the disk period (i.e., close to the star, or r_D small), the disk and the star have comparable periods, and the flare loop can be either trailing or leading. When the difference between the star and disk periods becomes large enough (r_D large), the star must rotate much faster than the disk, and only the trailing solution remains. The limiting cases of the asymptotes are when the disk is at infinity (then $P_* = P_{beat}$), or when the star does not rotate (then $P_{disk} = P_{beat}$). The question now becomes: in which regime are we?

⁴Such a situation had been invoked in the past to explain spectral features of classical T Tauri stars, such as emission lines and veiling, in terms of a boundary layer between a slowly rotating star and an accretion disk rotating at (fast) Keplerian velocities in contact with the star (see Bertout, Basri & Bouvier 1988).

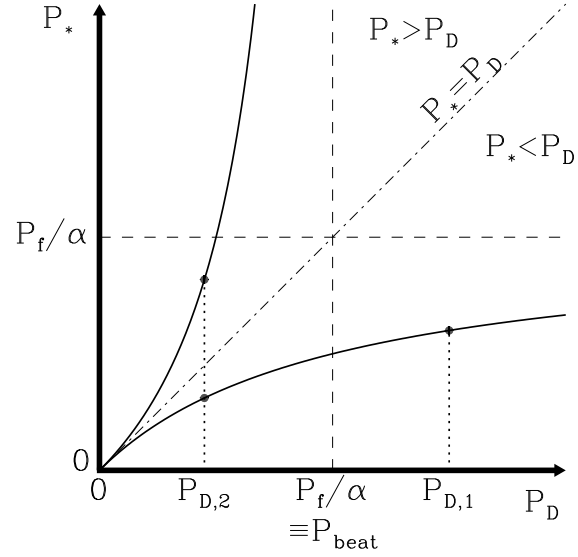


Fig. 3.— Stellar period (P_*) as a function of disk period (P_D). The possible solutions are in the form of two half hyperbolae, with asymptotes at $P_* = P_{beat}$ and $P_D = P_{beat}$. For $P_D = P_{D,2} < P_{beat}$, there are two solutions: one corresponds to $P_* < P_{D,2}$ (the star rotates faster than the disk), the other to $P_* > P_{D,2}$ (the disk rotates faster than the star). For $P_D = P_{D,1} > P_{beat}$, there is only one solution, with $P_* < P_{D,1}$.

For a star of mass M_* , the disk Keplerian rotation period P_D at B is:

$$P_D = 2\pi r_D^{3/2} (GM_*)^{-1/2}, \quad (4)$$

recalling that $r_D \approx R_* + 2R_{loop}$. We will use below (§4) a “mass-radius” relation between M_* and R_* , and find that the bolometric luminosity constrains the stellar mass to be $M_* \lesssim 2.2M_\odot$ (hence $R_* \sim 4.2R_\odot$). Thus, r_D being a function of R_* , we find via Eq. (4) P_D as a function of M_* only: this is shown on Fig. 4. Fixing $M_* = 2.2M_\odot$ yields $P_D \equiv P_{D,*} = 3.8$ days. In analogy with Eq. (1), we then define $\alpha_* \equiv P_f/P_{D,*} = 0.22$. Depending on whether α in Eq. (1) is smaller (resp. larger) than α_* , there will be two (resp. one) solution to Eq. (3).

We can now use results obtained in the framework of solar plasma physics. Amari et al. (1996) have made a 3D numerical simulation of the MHD evolution of a tubular magnetic loop anchored to footpoints twisted by some underlying movements (such as caused by convection on the solar surface). Their results demonstrate that it takes almost one twisting period τ_{twist} between the footpoints for field lines to begin to open: Fig. 4 of Amari et al. shows that the opening process is very slow at first, starting at $\approx 0.7\tau_{twist}$, then proceeds very fast. The field lines are completely open at $\sim 0.8\tau_{twist}$. Since the opening of field lines is a prerequisite for reconnection to occur at some later time τ_{rec} , we rewrite this result in the form $\tau_{rec} = \alpha_{rec}\tau_{twist}$, with the “reconnection parameter” $\alpha_{rec} \sim 0.8 - 1$: by doing so, we allow for a small random flare-to-flare change ($\leq 20\%$) in the moment when reconnection actually occurs, after the start of the opening of the field lines.

In YLW15, the X-ray flaring is produced by a star-disk shearing process having a characteristic time scale which is the relative period between the star and the disk, i.e., P_{beat} ; It is clear that the corresponding magnetic configuration (Fig. 2) is not the configuration of Amari et al.

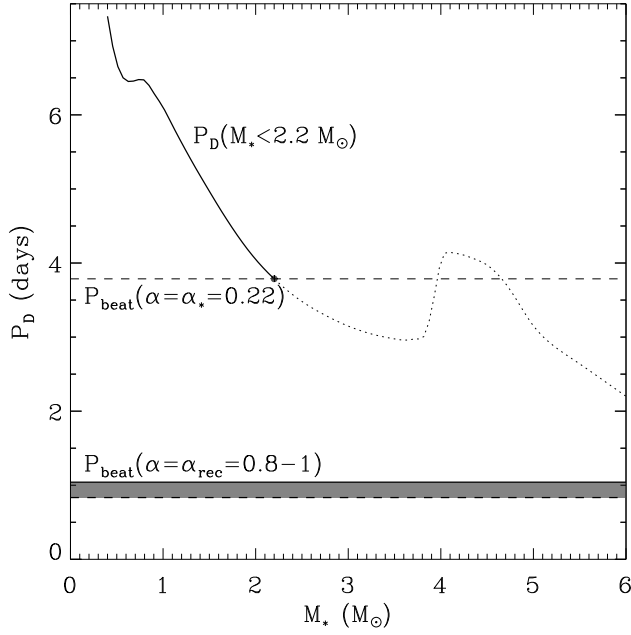


Fig. 4.— Comparison between the estimated disk period (P_D) and the star-disk beat period (P_{beat}). P_D is a function of the stellar mass (M_*), the stellar radius (R_*), and the flaring loop size. Using a “mass-radius” relation, and keeping the flaring loop size fixed (estimated in Paper I), P_D becomes a function of M_* only (dotted line). For YLW15, the bolometric luminosity gives an upper limit to the stellar mass of $M_* \sim 2.2 M_\odot$ (bold line; see text, §4), from which we obtain $P_D \equiv P_{D,*} = 3.8$ days. P_{beat} is proportional to the flare period P_f , via the parameter α ($P_{beat} = P_f/\alpha$). For $\alpha = \alpha_* \equiv P_f/P_{D,*} = 0.22$, $P_{beat} = P_{D,*}$, and there are two solutions for the stellar period: either the star does not rotate, or the star rotates with $P_* = P_{beat}/2$. On the other hand, solar plasma physics tell us (see discussion in the text, §2.1.3) that the “reconnection parameter” α_{rec} , characterizing the moment when flare ignition occurs after magnetic stresses are applied, is $\alpha_{rec} = 0.8 - 1$. The corresponding beat periods are respectively indicated by a continuous and a dashed horizontal lines, separated by a grey strip. Since $\alpha_{rec} > \alpha_*$, there is finally only one solution, in which the star rotates faster than the disk.

However, their results suggest that reconnection happens at the very end of the stress build-up process which has a characteristic time scale: P_{beat} in our case, τ_{twist} in the case of Amari et al. It is thus reasonable to identify P_{beat} with τ_{twist} and P_f with τ_{rec} . Then Eq. (1) can be understood as expressing the time lag separating the start of shearing process between the star and the disk, and the moment of flare ignition. Therefore, the parameter to be compared to α_* is $\alpha_{rec} \equiv P_f/P_{beat}$. With $\alpha_* = 0.22$, we find that $\alpha_{rec} > \alpha_*$.

We conclude that we are in the regime where there is only one solution, that of a star rotating faster than the disk. As illustrated on Fig. 4, $\alpha_{rec} > \alpha_*$ throughout the allowed stellar mass range, and the difference between α_{rec} and α_* is so large that this conclusion weakly depends on the actual value of α_{rec} , although the resulting stellar period P_* admittedly depends on it (via P_{beat}). For $\alpha_{rec} = 0.8 - 1$ as argued above, we find from Eq. (4) $P_* = 20 - 16$ h. In other words, *the central star of YLW15 must be a fast rotator*, having a rotation period shorter than the observed X-ray flare period, far from corotation with the inner part of the disk, which rotates much more slowly.

2.2. Magnetic braking

The situation in YLW15 is therefore *not* the “classical” quasi steady-state situation argued to hold in protostars (e.g., Shu et al. 1997) or in T Tauri stars (Königl 1991), but rather *precedes it*. The framework is reminiscent of disk-fed compact X-ray binaries, where a magnetized neutron star accretes material from a companion via a disk (see, e.g., Aly 1986 for an extensive review).

In the steady-state approximation, the magnetic field rotates as a solid body tied to the star, basically up to the Alfvén radius r_A where the ram pressure from the disk accretion flow (at a rate \dot{M}_{acc}) is balanced by the magnetic pressure. The basic idea, first proposed by Ghosh & Lamb (1978) for a neutron star having a dipolar magnetic field and surrounded by an infinitely thin accretion disk, is that the pressure of the inwards-moving material keeps field lines open down to a radius comparable to r_A . Conversely, the magnetic pressure inside this radius is strong enough to prevent the accreting material in the disk plane from spiralling in towards the star, but rather lifts it into free fall along the field lines. This concept of “magnetospheric accretion” in classical T Tauri stars (review by Shu 2000) has now been successfully modeled to interpret line emission features (e.g., Edwards et al. 1994; Muzerolle, Hartmann, & Calvet 1998), photometric variations (Bouvier et al. 1999), as well as the broadening of some absorption lines (Johns-Krull, Valenti, & Koresko 1999). The border region between the closed magnetosphere and the disk is in reality poorly known, with differential rotation and complex exchanges of angular momentum between the star and the disk, and depending strongly on the assumed magnetic diffusivity of the accretion disk, i.e., on the way the stellar magnetic field will actually penetrate the disk material.

Pursuing this issue further is beyond the scope of this paper. We will now simply follow the classic concept of “magnetic braking” to describe the *long-term evolution* of the star-disk system in the idealized situation where the inner border of the disk is located near the Alfvén radius, asymptotically ending up in “magnetic locking”, where the star and the inner disk corotate via a rigid magnetosphere (see, e.g., the details of the model by Shu et al. 1997) as is presumably the case in classical T Tauri stars (see below, §2.4).

In the above framework, the characteristic magnetic braking time scale t_{br} is obtained by equating the angular momentum variation and the magnetic torque (e.g., Königl 1991, and references therein):

$$d(J_* \Omega_*)/dt \sim \mu_*^2/r_A^3, \quad (5)$$

with $r_A = \beta \mu_*^{4/7} (2GM_*)^{-1/7} \dot{M}_{acc}^{-2/7}$ for a dipolar magnetic field.

The factor β takes into account the geometry of the accretion: $\beta = 1$ for spherical accretion, and $\beta = 0.52$ for accretion from an infinitely thin disk (Ghosh & Lamb 1979). In the case of protostars and T Tauri stars, however, the disk is rather geometrically thick (see the “flared disk” models introduced by Kenyon & Hartmann 1987, and the state-of-the-art observational constraints by Bell et al. 1997), and protostars also have circumstellar envelopes and outflows. Any distant coupling between the magnetic field and matter will make β tend towards 1: in fact, in some accreting neutron stars β has actually been *measured* to be ~ 1 (Wang 1996). As a result, for protostars it is likely that $\beta \lesssim 1$.

From Eq. (5), the braking time t_{br} can then be expressed as:

$$t_{br} \sim \beta^3 J_* \Omega_* \mu_*^{-2/7} (2GM_*)^{-3/7} \dot{M}_{acc}^{-6/7}, \quad (6)$$

where $J_* = \gamma(M_*)M_*R_*^2$ and $\mu_* = B_*R_*^3$ are respectively the moment of inertia and the magnetic moment of a star of mass M_* , radius R_* , and surface magnetic field B_* . For young stars at the “birthline”, the coefficient $\gamma(M_*) \simeq 1$ for masses in the range $M_* \sim 1 - 3 M_\odot$ (Palla 1999, priv. comm.; from the models of Palla & Stahler 1992), so that

$$t_{br} \sim (2G)^{-3/7} \beta^3 \Omega_* B_*^{-2/7} M_*^{4/7} R_*^{8/7} \dot{M}_{acc}^{-6/7}. \quad (7)$$

If the initial angular velocity is the break-up angular velocity $\Omega_{*,0} = (GM_*)^{1/2} R_*^{-3/2}$, the corresponding breaking time $t_{br,0}$ is

$$t_{br,0} \sim 2^{-3/7} G^{1/14} \beta^3 B_*^{-2/7} M_*^{15/14} R_*^{-5/14} \dot{M}_{acc}^{-6/7}. \quad (8)$$

Therefore $t_{br,0}$ is almost proportional to the stellar mass, almost inversely proportional to the accretion rate, but depends comparatively weakly on B_* and R_* .

For YLW15, the X-ray flare modelling gave a uniform equipartition magnetic field strength $B_{eq} \sim 150$ G. It is not completely clear to what extent the magnetic loop deduced from this flare could be related to some underlying large-scale magnetic structure. Assuming for simplicity that this structure is a dipolar magnetosphere, B_{eq} would be a measure of the value at the top of a dipolar loop, in which case the photospheric flux B_* would be more like ≈ 1 kG. In view of the uncertainties, we take $B_* \sim 0.1 - 1$ kG. As regards the relevant accretion rate, we will argue below (§4) that it is *not* the accretion rate necessary to build up the star ($\approx 1 M_\odot$ in $\approx 10^5$ yrs, i.e., $\dot{M}_{acc,*} \sim 10^{-5} M_\odot \text{ yr}^{-1}$; see Palla & Stahler 1992), which corresponds to the Class 0 protostar phase, but rather the presently observed Class I disk accretion rate deduced from the outflow or the bolometric luminosity, which is about 10 times smaller. Thus within a factor of < 2 if β lies between $\beta \sim 0.75$ (see below, §5.1) and $\beta = 1$, we express $t_{br,0}$ numerically as

$$t_{br,0} \sim 3.3 - 7 \times 10^5 \text{ yrs} \times \left(\frac{B_*}{1000 \text{ G}} \right)^{-2/7} \left(\frac{R_*}{R_\odot} \right)^{-5/14} \times \left(\frac{M_*}{M_\odot} \right)^{15/14} \left(\frac{\dot{M}_{acc}}{10^{-6} M_\odot \text{ yr}^{-1}} \right)^{-6/7}. \quad (9)$$

Taking $M_* \approx 2 M_\odot$, and $R_* \approx 4 R_\odot$ from the models by Palla & Stahler (1992) for the central star of YLW15 (see §4), and the above values for the other parameters, we find $t_{br,0} \sim 4.3 - 17 \times 10^5$ yrs for $B_* \sim 1 - 0.1$ kG and $\beta \sim 0.8 - 1$. With a build-up accretion rate $\dot{M}_{acc,*} \sim 10^{-5} M_\odot \text{ yr}^{-1}$, the age of YLW15 is $\sim 2 \times 10^5$ yrs, i.e., smaller than $t_{br,0}$. This suggests that the central star of YLW15 is still decelerating, and has not yet been brought to a steady-state corotation with the inner part of the accretion disk. (We neglect here any possible deceleration having taken place during the earlier Class 0 stage, which, lasting $\sim 10^4$ yrs [AWB], is very short. In addition, at this stage there is no “real” star, but mainly an infalling rotating envelope [see, e.g., Terebey, Shu, & Cassen 1984], so that angular momentum may actually be *gained* during this phase; see also the discussion in §6. In addition, we have no idea of the magnetic field origin, configuration, or intensity at this stage, so that Eq. [9] cannot be applied anyway.)

As a final consistency check between the long-term evolution given by t_{br} and the short-term magnetic shearing leading

to reconnection, we must verify that the Alfvén radius r_A is not larger than the disk radius at footpoint B , r_D ($\sim 3.5 R_*$). We find numerically:

$$r_A = 1.1 R_\odot \times \beta \left(\frac{B_*}{1000 \text{ G}} \right)^{-4/7} \left(\frac{R_*}{R_\odot} \right)^{-12/7} \times \left(\frac{M_*}{M_\odot} \right)^{-1/7} \left(\frac{\dot{M}_{acc}}{10^{-6} M_\odot \text{ yr}^{-1}} \right)^{-2/7}. \quad (10)$$

We thus have $r_A \lesssim r_D$ for $B_* \lesssim 950 - 1900$ G ($\beta = 0.5 - 1$), which is compatible with the X-ray derived values of B_* .

2.3. A collimated coronal wind ?

In our case, as a consequence of the assumed X-ray-induced strong magnetic coupling between the star and the disk, there is no rigid magnetosphere, but rather a succession of readjustments via shearing and reconnection. There will be energy losses and momentum exchanges between the star and the disk, leading to “magnetic braking”. Energetic X-ray flares can be taken as a tracer of the energy lost in radiative form during this braking (see below). In solar flares and other manifestations of coronal activity, material is ejected after reconnection events by a variety of processes. So we expect the star to eject material in some form of *coronal wind*. We can obtain an order-of-magnitude estimate of the corresponding mass-loss rate during a flare such as the ones discussed here by assuming that this wind comes from the plasma “rings” left after reconnection, in a fashion analogous to solar coronal mass ejections. The mass of this detached part, approximated by a ring of radius R_{ring} and cross-section diameter $2\pi R_{ring} \times a$, will be

$$m_{ej} \approx 2\pi R_{ring} \times \pi^3 a^2 R_{ring}^2 \times n_e m_p = 2\pi^4 a^2 R_{ring}^3 n_e m_p. \quad (11)$$

Taking Fig. 2 at face value, we adopt $R_{ring} \approx R_* + R_{loop} \approx 8.7 R_\odot$. Also (Paper I), the aspect ratio $a = 0.07$, and the plasma density $n_e = 5 \times 10^{10} \text{ cm}^{-3}$. We thus find $m_{ej} = 1.8 \times 10^{22} \text{ g}$ per flare event. Taking this mass to be ejected every $P_f \sim 20$ h, the resulting mass-loss rate is $\dot{M}_{ej} = m_{ej}/P_f \sim 3.9 \times 10^{-9} M_\odot \text{ yr}^{-1}$. However, it is important here to realize that such a coronal wind *should not be confused* with the outflows currently associated with protostars, which have a mass-loss rate several orders of magnitude larger ($\dot{M}_{out} \approx 10^{-5} M_\odot \text{ yr}^{-1}$ for Class I protostars, see Bontemps et al. 1996). In most models, such outflows result from a (cold) *disk* wind, completely distinct from what happens in the vicinity of the central star inside the Alfvén radius (e.g., Camenzind 1997, Königl & Pudritz 2000).

If this order of magnitude for \dot{M}_{ej} is correct, then we should worry about a number of consequences.

(i) Being free from star and disk material, the magnetic ring will not confine the plasma anymore, which will therefore expand and cool via radiative and adiabatic losses; based on the analogy with the solar wind, heating (for instance by Alfvén waves) may also happen. We can speculate that the equilibrium temperature will be a “typical” coronal temperature $T_e \sim 10^6$ K. As a result, the plasma will radiate in soft X-rays ($\lesssim 0.1$ keV), which are totally absorbed by the intervening material, hence be undetectable.

(ii) However, *this plasma will also radiate in the centimeter radio range*, which suffers no extinction by the surrounding

matter unless this matter is fully ionized. We have mentioned in the Introduction (§1) that YLW15 is the seat of the highest radio emission, likely thermal, of all the VLA sources in the ρ Oph core F, with a total flux density $F_{5\text{GHz}} = 3.3$ mJy. It is thus tempting to compare this value with the free-free emission from the putative coronal wind of YLW15.

The scenario illustrated in Fig. 2 suggests that we are dealing with a bipolar geometry. Then, for a standard ionized wind of temperature T_e , contained in a cone of aperture θ_0 inclined at an angle i to the observer, and flowing at velocity v_w , the mass-loss rate \dot{M}_{ej} corresponding to a free-free radio flux density F_ν at frequency ν is given by (from Reynolds 1986, André 1987; for $\theta_0 \lesssim 0.5$):

$$\begin{aligned} \dot{M}_{ej} = & 5.2 \times 10^{-9} M_\odot \text{yr}^{-1} \theta_0^{3/4} (\sin i)^{-1/4} \left(\frac{F_\nu}{\text{mJy}} \right)^{3/4} \\ & \times \left(\frac{v_w}{100 \text{ km/s}} \right) \left(\frac{\nu}{5 \text{ GHz}} \right)^{-0.45} \left(\frac{T_e}{10^4 \text{ K}} \right)^{-0.075} \\ & \times \left(\frac{d}{160 \text{ pc}} \right)^{1.5}. \end{aligned} \quad (12)$$

Strictly speaking, this relation is valid for $kT_e \lesssim 0.05$ keV; above this value, quantum effects become important, but the temperature dependence of the emissivity retains a logarithmic term (Oster 1961), so that for simplicity we will keep the same equation for kT_e up to $\sim 0.1 - 1$ keV. In Eq. (12) above, the plasma temperature plays in practice a very small role, which is fortunate because we do not know the actual temperature structure of the coronal wind. For YLW15, we can take $\sin i = 1$, $v_w \approx 300 \text{ km s}^{-1}$ (escape velocity from the surface of the central star), and we adopt $T_e = 10^6 \text{ K}$. We know all the other parameters, except the opening angle θ_0 . Gathering numbers, we find:

$$\theta_0(\text{YLW15}) = 0.012 \left(\frac{\dot{M}_{ej}}{10^{-9} M_\odot \text{yr}^{-1}} \right)^{4/3}, \quad (13)$$

which, taking the value of \dot{M}_{ej} we have derived, gives $\theta_0 = 0.08$, or about 5° . This good collimation (in reality a conical approximation to the actual wind flow) suggests that such a coronal wind could be related to the jets frequently seen in the close vicinity of YSOs (e.g., Rodríguez 1997).

(iii) Making VLBI observations of YLW15, André et al. (1992) determined that the radio-emitting region should be $\gtrsim 1$ AU in size. Then we should worry that, since we know that the source is variable in X-rays (see also below, §5.2), the radio-emitting plasma may live long enough against recombination that it keeps a good chance to be detected in case the star-disk magnetic source is cut off. The recombination coefficient of a plasma having $kT_e > 0.05$ keV is $\alpha_r = 3.5 \times 10^{-15} (Z + 1)^2 I_Z^{1/2} (kT_e)^{-1} \text{ cm}^{-3} \text{ s}^{-1}$ (Z = ion charge, I_Z = ionization potential, energies in keV), so that for hydrogen the recombination time is $t_r = 1/(\alpha_r n_e) = 6.1 \times 10^4 \text{ s} \times (kT_e/\text{keV}) (n_e/10^{10} \text{ cm}^{-3})^{-1}$. At the base of the cone, near the star, the density is high and the recombination time is short; however, for a constant velocity wind, $n_e(r) \propto r^{-2}$, and lower densities dominate the emitting volume. Taking $n_e = 5 \times 10^{10} \text{ cm}^{-3}$ at $r = R_{\text{loop}}$, we find at $\gtrsim 1$ AU $n_e = 2 \times 10^7 \text{ cm}^{-3}$, and $t_r \gtrsim 3 \times 10^6 \text{ s}$, or $\gtrsim 1$ month.

(iv) Finally, travelling at $v_w \sim 300 \text{ km s}^{-1}$, the plasma will reach $r \gtrsim 1$ AU in $\gtrsim 6$ days, i.e., more than 7 X-ray periods: therefore *we do not expect the radio emission of YLW15 to be variable on \sim day time scales, i.e., to carry any signature of the underlying stellar rotation*. On the other hand, the emission will look continuous (or perhaps weakly variable) as long as the magnetic shearing process giving rise to the X-rays does not stop for more than $\gtrsim 1$ month at a time. All we can say at this point is that these conditions do not seem unreasonable.

We thus conclude that collimated hot coronal winds such as the one we have invoked for YLW15 must contribute to the thermal radio emission of protostars, and may perhaps even explain it. In this case, what is commonly referred to as “the ionized base of the outflow” (or of the jets) to interpret the radio emission, implying in particular temperatures $\sim 10^4 \text{ K}$ which are unexplained so far, may rather be in reality AU-sized bipolar “coronal winds” at $\sim 10^6 \text{ K}$, originating in magnetic interactions between the star and the disk.

On the other hand, it may look surprising that we have not so far considered *non-thermal* radio emission related to X-ray flares, since gyrosynchrotron emission has been detected in a number of YSOs, and is directly tracing, like the X-rays, their magnetic activity (FM). However, it turns out that, contrary to thermal emission, detections of non-thermal emission are extremely rare for protostars. The only *bona fide* case is that of the X-ray emitting Class I protostar R CrA IRS5, which has been seen with the VLA to emit a strongly circularly polarized radio flux (Feigelson, Carkner, & Wilking 1998). Remarkably, the radio emission is variable on a time scale of ~ 1 day at a level 0.15 – 0.45 mJy. This variability could perhaps be related to the break-up period of the central object: indeed, on the birth-line the break-up period is comprised between ~ 13 h and ~ 33 h for $M_\star \lesssim 5 M_\odot$ (see §4 and Fig. 6 below). Gyrosynchrotron radio emission does have, like X-ray flares, and contrary to the thermal emission, the potential to carry the signature of some characteristic time scale tracing a stellar period. However, this emission is easily absorbed by intervening fully ionized material (including the coronal wind itself), and it seems that it can be detected only in very favourable circumstances (temporarily lower mass loss, particularly efficient electron acceleration, geometry, etc.).

2.4. Energy storage vs. energy release

Turning to the *maximum* magnetic power which can be stored in the star-disk system with a magnetic structure explaining the observed flares of size $\approx r_D \approx r_A$, we have

$$(dE_{\text{mag}}/dt)_{\text{max}} \sim |\Omega_\star - \Omega_D| \mu_\star^2 / r_D^3 \approx \Omega_\star \mu_\star^2 / r_D^3, \quad (14)$$

(see, e.g., Shu et al. 1997). With the above parameters for YLW15, we find $(dE_{\text{mag}}/dt)_{\text{max}} \sim 10^{36} \text{ erg s}^{-1}$. Equivalently, over one period of $\lesssim 1$ day, $E_{\text{mag}} \lesssim 10^{41} \text{ erg}$ can be released, which shows that an enormous amount of magnetic energy is accumulated, at the expense of the star-disk differential rotation. The total energy released by the “superflare” detected in YLW15 with ROSAT by Grosso et al. (1997) is $E_{\text{tot}} \approx 10^{37-38} \text{ erg}$, which suggests that such extremely energetic events can *only* be explained by star-disk magnetic reconnection phenomena. There is of course no difficulty to explain lesser (but still intense) flares like the quasi-periodic flares detected with ASCA, for which E_{tot} is $\lesssim 1$ order of

magnitude smaller, since a large fraction of the total luminosity may be emitted at lower temperatures in the form of optical/UV/soft X-ray photons which would be more easily absorbed by intervening material than at the \sim few keV seen by ASCA. Also, another fraction of the power will be kinetic: for instance, the coronal wind discussed in the preceding section has $dE_c/dt = \frac{1}{2}\dot{M}_{ej}v_w^2 \sim 10^{32}$ erg s $^{-1}$. In addition, some of the power may go into particle acceleration (see FM).

On the other hand, X-ray “superflares” of the intensity of YLW15 have never been observed on any of the several hundred X-ray detected T Tauri stars, which implies for them $(dE_{mag}/dt)_{max} = 0$ in Eq. (14) above. In turn, this implies either $\Omega_\star = \Omega_D$, or $r_D \rightarrow \infty$. The first case must then apply to classical T Tauri stars (CTTS), while the second corresponds to “weak-line” T Tauri stars (WTTS, or “Class III” sources), which have no disk (or at least no disk interacting with the central star). Strictly speaking, this means that the only magnetic activity left for T Tauri stars is their solar-like activity, which should then be essentially identical for CTTS and WTTS, irrespective of the presence or absence of a disk.

This is fully consistent with observations: the X-ray emission properties from CTTS and WTTS are essentially indistinguishable, and their X-ray activity bears all the symptoms of being solar-like, with no indication of the presence of a disk playing any role (see FM). More precisely, at least as far as X-ray diagnostics are concerned, in spite of the fact that magnetic reconnections may conceivably take place between the star and the disk, or even within the disk itself (see FM; and also Aly & Kuipers 1990), observations of classical T Tauri stars show that these reconnection events must be much less important than stellar solar-like magnetic activity. (However, it cannot be excluded that such events generate lower-temperature flares, which would emit EUV radiation easily absorbed by the intervening material, and/or be undetectable by X-ray satellites.)

We conclude that extreme X-ray luminosities are never released at the T Tauri stage because a significant change of star-disk magnetic configuration leading to reconnection has become impossible: in the case of CTTS, the magnetosphere and the inner boundary of the disk are somehow bound together in solid rotation as a result of magnetic braking, and possible magnetic interactions within the disk beyond this boundary must be comparatively small. At this later stage, magnetic reconnection events leading to the observed X-ray flares are therefore only those resulting from convective movements at the stellar surface, as they are in the case of WTTS, where the disk is absent.

3. WL6: A SLOWLY ROTATING PROTOSTAR

Kamata et al. (1997) present an ASCA observation of another Class I protostar in the ρ Oph cloud, WL6 (Wilking & Lada 1983), also known as YLW14, spread over ~ 20 h. They give a sinusoidal fit to the light curve, but actually only about 3/4 of such a sinusoid is seen. These authors propose that the variation is really periodic, with a period $P_\star = 0.97$ day, and attribute it to a rotating large active region at the stellar surface. We note however that a strictly sinusoidal behavior is not compatible with an eclipse phenomenon, whether it refers to a rotating active region, to a binary system, or more generally to some external occultation (see for instance the periodic, but highly non-sinusoidal X-ray light curve of the O7 star θ^1 C Ori interpreted in terms of disk occultation by Babel & Montmerle 1997).

We have therefore reexamined the observation of Kamata et

al. in the light of the recent work on rotational modulation of X-ray flares by Stelzer et al. (1999), which gives a new interpretation of “slowly” rising and decaying light curves similar to that observed in WL6. The idea, first proposed by Casanova (1994) for the ρ Oph CTTS SR12, is that an X-ray flare has occurred on the back side of the star prior to the beginning of the observation, and that the observation starts during the cooling phase, while the magnetic loop confining the plasma appears above the limb and comes into view. For WL6, the X-ray temperature behavior along the light curve apparently does not change significantly, being successively (after rebinning into two time intervals) kT_X (keV) = $2.2(+0.5/-0.4)$, and $2.2(+1.0/-0.6)$, but the uncertainties are large, so we concentrate on the light curve. We model it as in Stelzer et al., with 6 parameters: maximum intensity, quiescent level, e-folding cooling time, start of flare egress above the horizon, stellar period, and radius of the loop. Figure 5 shows the result. We find that the data can be fit in particular with a comparatively small equatorial plasma bubble (radius/ $R_\star \sim 0.8$), and a *slow rotation* ($P_\star = 3.3$ days), much slower than inferred from the sinusoidal fit. The reduced χ^2 is 1.3 for 12 degrees of freedom, which is comparable to the sinusoidal fit ($\chi^2 = 1.1$ for 14 degrees of freedom). The light curve of WL6 can be compared to the light curve of YLW15 (see Fig. 1).

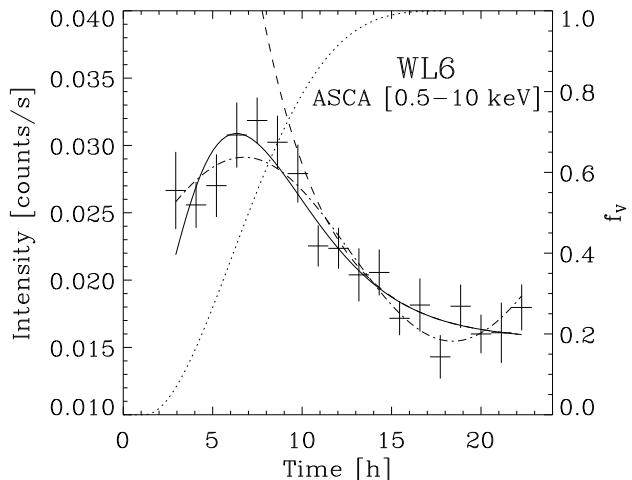


Fig. 5.— Light curve of WL6 obtained with ASCA (Kamata et al. 1997), reexamined in the framework of the rotational modulation of a spherical flare starting on the back of the star (Stelzer et al. 1999). The fitted parameters of the continuous line are: quiescent level ($= 0.016$ cts s $^{-1}$); flare maximum ($= 0.110$ cts s $^{-1}$); flare cooling timescale ($\tau = 3.6$ h); moment of egress after the start of the observation ($t_{egress} = 1.2$ h); plasma volume fraction f_v ($=$ visible volume/final volume) as a function of time, as seen by the observer, indicated by the dotted line; stellar period ($P_\star = 3.3$ days); and ratio between the plasma sphere radius and the stellar radius ($f = 0.76$). The reduced $\chi^2 = 1.3$ for 12 d.o.f. The dashed line shows the flare cooling phase without the rotational modulation. The dot-dashed line is the sinusoidal fit by Kamata et al. 1997 (reduced $\chi^2 = 1.1$ for 14 d.o.f.). Note the difference with YLW15 (see Fig. 1) in terms of luminosity (count rate on the left vertical scale) and duration (horizontal scale).

At this point, it is important to emphasize that while being also classified as a Class I protostar on the basis of its IR properties, WL6 is a quite different object from YLW15. Situated near the B1/B2 core region, it is not embedded in a large condensation like YLW15, but rather appears isolated (MAN). Its bolometric luminosity is $L_{bol} \sim 1.1 L_\odot$ (Lada & Wilking 1984).

While its rising slope at short wavelengths, with $\alpha_{IR}(2-10\mu\text{m}) = 1.0$, formally makes it a Class I protostar, its SED is essentially flat beyond $3.4\mu\text{m}$, so that it rather belongs to the “flat-spectrum”, or embedded T Tauri, category. In fact, a classical T Tauri star with an edge-on disk could perhaps give a better interpretation of this kind of SED (see, e.g., Chiang & Goldreich 1999), and would give additional support to our interpretation of the X-ray light curve in terms of an equatorial rotationally modulated flare. No circumstellar envelope could be detected in the millimeter observations by AM and MAN: this yields an upper limit to the envelope mass $M_{\text{env}} \lesssim 10^{-3} M_{\odot}$. An outflow weaker than the one of YLW15 has been detected by Sekimoto et al. (1997). From these characteristics, *WL6 appears as significantly more evolved than YLW15*. In addition, no VLA emission has been detected, down to a very low limit ($F_{5\text{GHz}} < 100 \mu\text{Jy}$, i.e., ~ 30 times less than for YLW15). In spite of its isolation away from the ρ Oph dense cores and its small envelope, its extinction, classically derived from near-IR data, is high: taking the recent near-IR data by Barsony et al. (1997) and assuming a flat-spectrum disk with an intrinsic $H-K = 0.9$, we find $A_{V,IR} \sim 40$; a lower value has been found from the X-rays: $A_{V,X} \sim 20$. This would be consistent with an edge-on disk, again invoking a lower gas-to-dust ratio than usual (grain condensation in the disk?). Uncertainties on A_V are clearly large anyway.

Choosing $A_V \sim 20$ for consistency with the X-ray data, the maximum (hidden) luminosity given by the rotationally modulated flare model is then ~ 3.8 times higher than the value derived by Kamata et al., to become $L_{X,\text{max}}[2-10\text{keV}] \sim 5.3 \times 10^{31} \text{ erg s}^{-1}$.

This luminosity value is high compared to the average X-ray luminosity of T Tauri stars ($L_X \simeq 3 \times 10^{28} - 3 \times 10^{29} \text{ erg s}^{-1}$, see FM), and only 4–20 times less luminous than the unusually strong X-ray flare recently observed on the weak T Tauri star V773 Tau (Skinner et al. 1997; also studied by Stelzer et al. in terms of rotational modulation), for which a comparable rotation period is obtained. This suggests that the central star of WL6 behaves in X-rays more like an “extreme” T Tauri star, rather than as a protostar like YLW15, owing to its much slower rotation. *This is consistent with its status independently deduced from IR and mm observations*. In that case, the WL6 X-ray flare would be due to (enhanced) solar-like activity on its surface, rather than to star-disk interactions. This conclusion is also consistent with the absence of detectable cm radio emission.

4. STELLAR PARAMETERS FOR YLW15 AND WL6

In the preceding sections, we had to use estimates of stellar parameters such as the radius or the mass, and the accretion rate. *Stricto sensu*, at the Class I stage these quantities are rather ill-defined theoretically and cannot be measured directly. Class I characteristics are derived from the envelope (mainly via its SED), not by the central object. However, the X-ray behaviour of YLW15 and other X-ray detected protostars strongly suggest that a genuine stellar object, with a photospheric radius and a mass, is present inside the circumstellar envelope of Class I protostars.

To refine our previous estimates, we therefore make the step to consider that YLW15 and WL6 are very close to their “birthlines” (e.g., Stahler 1988) where they become optically visible, at least as far as the *stellar* properties are concerned. Even if the envelope properties of YLW15 suggest that it has not

quite reached that stage, the envelope mass determined from mm measurements (§1) is $\ll 1 M_{\odot}$, which implies that the central object has indeed essentially reached its final mass. This is even more true for WL6, which does not have a detectable envelope.

We can then use the models by Palla & Stahler (1992, 1993; hereafter PS) which define a “protostar mass-radius relation” (hereafter the PS relation) as a function of the accretion rate $\dot{M}_{\text{acc},*} \sim a^3/G$ (where a is the sound speed in the dense core; e.g., Shu, Adams, & Lizano 1987) building up the star. The standard value (for dense cores with temperatures $\sim 30\text{ K}$) is $\dot{M}_{\text{acc},*} \sim 10^{-5} M_{\odot} \text{ yr}^{-1}$ (Adams, Lada, & Shu 1987).

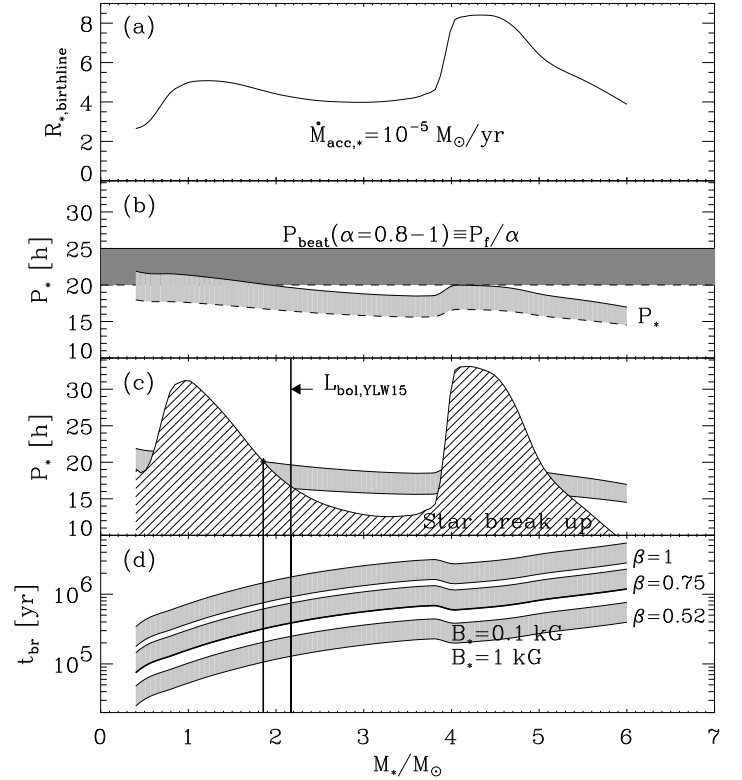


Fig. 6.— (a) Mass-radius relation assuming a star build-up accretion rate, $\dot{M}_{\text{acc},*} = 10^{-5} M_{\odot}/\text{yr}$, on the “birthline” (Stahler 1988 for $M_* < 1.5 M_{\odot}$; Palla & Stahler 1992 for higher masses). (b) Relation between the rotation period of YLW15, P_* (calculated from the flare period, the magnetic loop size of the YLW15 X-ray flares, and the mass-radius relation shown on the first panel), and the beat period, P_{beat} , deduced from the flare period, assuming the relation $P_{\text{beat}} = P_f/\alpha$ (dashed line: $\alpha = 1$; continuous line: $\alpha = 0.8$). The grey strip shows the computed values of the star rotation period for $\alpha = 0.8 - 1$ (see text, §2.1.3; same strip as shown in Fig. 4). (c) Corresponding break-up period as a function of stellar mass, and forbidden periods underlined by the shaded area (period shorter than the break-up period). The right vertical line corresponds to the upper limit to the mass of YLW15 deduced from its observed bolometric luminosity (see text, §4); the left vertical line is the lower limit derived from the rotation constraints (panel 3). (d) Braking time t_{br} as a function of mass (and radius via the mass-radius relation shown on panel a) for a disk accretion rate $\dot{M}_{\text{acc}} = 10^{-6} M_{\odot}/\text{yr}$, three values of β describing the accretion geometry ($\beta = 0.52$ for a geometrically thin accretion disk, $\beta = 1$ for spherical accretion), and two values of the photospheric magnetic field B_* (0.1 kG, and 1 kG). For reference, the duration of the Class I stage is estimated at $0.75 - 1.5 \times 10^5 \text{ yr}$ (Luhman & Rieke 1999). The thick curve ($B_* \sim 1 \text{ kG}$, $\beta \sim 0.75$) is our “best choice” to explain at the same time the fast rotation of YLW15 and the slow rotation of WL6. We see

that the braking time is then shorter than the age of Class I protostars for masses smaller than $\approx 1 - 2M_\odot$.

PS also find independently that a good fit to the observed locations of the youngest low- to intermediate- mass stars in the H-R diagram is obtained with this value of $\dot{M}_{acc,*}$. PS then derive two series of models, depending on the accretion mode, spherical or from a disk: given the young stage of YLW15 and WL6, we take the disk-accretion build-up model, and we will therefore use the corresponding PS relation (shown in Fig. 6a) in what follows.

On the other hand, outflow observations show evidence for a strong decrease in the accretion rate from the build-up stage (i.e., Class 0) to the Class I stage (end of build-up) (Bontemps et al. 1996), as shown by their evolutionary diagram plotting (F_{CO}/L_{bol}) vs. $(\dot{M}_{env}/L_{bol})^{0.6}$, where F_{CO} is the outflow momentum flux. Such observations are supported by some outflow models (see Henriksen, André, & Bontemps 1997 and references therein). In this diagram, the positions of YLW15 and WL6 suggest $\dot{M}_{acc} \approx 10^{-6} M_\odot/\text{yr}$. A low accretion rate of this order is also required at the Class I stage in order that the accretion luminosity $L_{acc} = GM_*\dot{M}_{acc}/R_*$ does not exceed the observed bolometric luminosity ($L_{bol} \sim 10 L_\odot$ for YLW15).

Let us discuss YLW15 in more detail. (i) Having the X-ray flare period, the size of the magnetic loop and the PS mass-radius relation, we find from Eq. (3) that the star rotation period must be smaller than the beat period (§2.1.3 above; see Fig. 6b). (ii) The equatorial velocity of YLW15 cannot exceed the break-up velocity, which translates into a limiting condition on the star rotation period, i.e., one must have $P_* > P_{*,0}$ (break-up period, illustrated in Fig. 6c), with permitted zones in the mass ranges $M_* \sim 1.8 - 4.0 M_\odot$ and $M_* \gtrsim 5 M_\odot$, as indicated by the hatched area. (iii) An independent constraint comes from the observed L_{bol} taken at the birthline: the photospheric luminosity $L_* = 4\pi R_*^2 \sigma T_{eff}^4$ should be at most equal to L_{bol} (any difference being attributable to the accretion luminosity): from the birthline on the H-R diagram (Palla & Stahler 1993), we find $M_* \leq 2.2 M_\odot$ (see Fig. 6c). Combining all these constraints, we conclude that the mass and radius of the central object of YLW15 must lie in the ranges $M_* = 1.8 - 2.2 M_\odot$, and $R_* = 4.6 - 4.2 R_\odot$ (PS relation). In other words, according to the above arguments, YLW15 must be a *future Herbig AeBe star*, itself the progenitor of an A star. It is noteworthy that this status then sets YLW15 apart from the typical, lower-mass YSO in the ρ Oph cloud, a fact that was already noticed in relation with some of its particular properties described in §1.

On the other hand, WL6, by way of its small luminosity ($L_{bol} = 1.1 L_\odot$) is necessarily a low-mass star ($M_* \lesssim 0.4 M_\odot$), with $R_* \lesssim 2.7 R_\odot$ (PS relation). Returning to the braking times (Eq. (10)), and adopting the same values of B_* , \dot{M}_{acc} and β as for YLW15, we find that for WL6 (assumed initially rotating at break-up, i.e., $P_{*,0} \sim 19$ h from PS) $t_{br,0}$ is at least 5 times (\sim the mass ratio) shorter than for YLW15. As a result, WL6 must have gone through most of its braking phase, so that its magnetic field is by now likely locked to the accretion disk. Comparing the rotation characteristics of YLW15 and WL6, we conclude that *YLW15 is a fast rotating protostar of intermediate mass, while WL6 is a spun-down low-mass protostar*.

5. DISCUSSION

5.1. A mass-rotation relation close to the birthline ?

More generally, Fig. 6d displays the magnetic braking timescale from initial break-up (Eq. 9) as a function of stellar mass. If the accretion rates and magnetic fields are the same for the high and the low stellar masses, we find that the rotational status of protostars is mainly governed by the stellar mass, unless other factors like B_* or the accretion geometry parameter β are very different from star to star. The X-ray observations certainly suggest that B_* should not vary much. Fig. 6d illustrates all the possible cases. However, using X-ray flaring as a clock, we have “measured” the rotation periods of YLW15 (fast) and WL6 (slow), and we have an estimate of their masses. In the absence of a better individual age determination for these protostars than an average value $\sim 1 - 2 \times 10^5$ yrs, we can then use their rotation properties to “normalize” the set of $t_{br} - M_*$ curves of Fig. 6d: we find that $B_* \sim 1$ kG and $\beta \sim 0.75$ is a reasonable combination (thick line). The value $B_* \sim 1$ kG is fully compatible with all the X-ray observations of YSOs (FM); the fact that $\beta \sim 0.75$, could be an indication that for Class I protostars the actual accretion geometry is a mixture of disk ($\beta = 0.52$) and spherical accretion ($\beta = 1$).

In these conditions, the critical mass M_{crit} such that, near the birthline, stars with $M_* > M_{crit}$ may be fast rotators (i.e. $t_{br,0} >$ lifetime) is $M_{crit} \approx 1 - 2 M_\odot$. This limit may not be very precise, however, because low-mass stars are clearly more affected by star-to-star variations of the various parameters entering Eq. (9), and also because individual stellar lifetimes are still uncertain.

This conclusion may be affected at a later stage during the evolution by a change in the accretion rate, suggested by outflow observations (see §4). For low-mass objects like WL6, which are braked quickly and are now slowly rotating, a late decline in the disk accretion \dot{M}_{acc} ($\sim 10^{-7} M_\odot \text{ yr}^{-1}$ at the T Tauri stage) has no consequence. However, like YLW15 higher-mass objects may end their Class I stage while still appreciably rotating: since t_{br} is approximately inversely proportional to \dot{M}_{acc} , the braking effect will essentially stop just before the birthline, and the star will continue to spin down but on much longer timescales. In other words, even some time after the birthline the rotation status will reflect the conditions on the birthline: taking into account the fact that the stellar mass turns out to be the most widely variable parameter in Eq. (9), our estimate of the magnetic braking time scale predicts a *mass-rotation relation* of the form $t_{br} \propto M_*$, where close to the birthline the stars should be slow rotators below $M_{crit} \approx 1 - 2 M_\odot$, and fast rotators above. Such a relation can also be considered as an initial condition for the rotation history of T Tauri stars.

Observationally, this could be an explanation for the existence of rapid rotators among very young stars: our prediction here is that rapid rotators should in general be relatively massive. There are some hints that this may be the case: the three rapid rotators ($P_* = 1.5 - 2$ days) among the list of classical T Tauri stars with measured rotation periods by Bouvier (1990) all have masses between 1.5 and $2.0 M_\odot$, and Herbig AeBe stars, which have masses $\sim 2 - 8 M_\odot$, seem, as a rule, to be fast rotators (Boehm & Catala 1995).

5.2. Fast stellar rotation vs. accretion

An intriguing paradox arises if the central star of YLW15 is really rotating near break-up. Indeed, in such conditions the presence of a strong magnetic field (enough to balance the incoming accretion flow at r_A) would inhibit accretion onto the central object and convert all the incoming material into an outflow, thereby preventing the star to form in the first place. This

shows that accretion and magnetic interactions cannot be steady phenomena: episodes dominated by star-disk magnetic interactions and (periodic) flaring must be separated by episodes of intense accretion, accompanied by different ejection phases. The succession of intense accretion episodes is reminiscent of the FU Orionis phenomenon, in which the accretion rate is so high ($\dot{M}_{acc} \approx 10^{-4} M_{\odot} \text{ yr}^{-1}$) that the star is engulfed by the disk (e.g., review by Hartmann, Kenyon, & Hartigan 1993). The corresponding duty cycle for protostars is unknown, but in the case of YLW15, we have already seen two different flaring regimes: a “high state”, with a superflare and a quasi-periodic flaring episode, as well as a “low state”, with a non-detection by ASCA on one previous occasion (Koyama et al. 1994; Kamata et al. 1997).

On the other hand, the existence of “high” and “low” X-ray activity states is reminiscent of the QPO phenomenon, and indeed the suggestion that episodic flaring may occur as a result of reconnection between a neutron star and its accretion disk has been suggested in the past (see Aly & Kuipers 1990). Alternatively, such a phenomenon might be explained in the framework of accretion instabilities in magnetized disks (Tagger & Pellat 1999). Other mechanisms may be invoked. For instance, it is known that X-rays ionize the accretion disk and, at least in T Tauri stars (where $\dot{M}_{acc} \approx 10^{-7} M_{\odot} \text{ yr}^{-1}$), may regulate the accretion rate via the (small-scale) Balbus-Hawley magnetorotational instability (Glassgold, Najita, & Igea 1997; Glassgold, Feigelson, & Montmerle 2000). One can then imagine a feedback mechanism based on the X-ray flares themselves: more X-rays means more ionization, and thus more accretion, which, if high enough, may engulf the magnetic field and stop the flaring, or at least absorb the X-rays near the star, so that the disk ionization drops, slowing the accretion flow and letting the X-ray flaring phase resume to start a new cycle.

Obviously this situation is new and complex, and detailed 3D calculations are needed to take into account the accretion, the magnetic field deformation preceding the reconnection, and possibly the feedback of X-rays on accretion. The ASCA observation of a triple X-ray flare reported in Paper I clearly forces us to reconsider the details of the mechanisms of accretion in forming, fast rotating stars.

5.3. Class I protostars: X-ray loud vs. X-ray quiet

The preceding discussion also suggests that rather stringent conditions must be met for a Class I protostar to have detectable X-ray emission. Given the high extinctions, the detectable X-ray luminosities are $L_X \gtrsim 10^{30-31} \text{ erg s}^{-1}$ at the level of sensitivity of ROSAT or ASCA, which is higher than the values corresponding to the usual solar-like activity seen on T Tauri stars. Thus, as argued in §2.4, it is likely that very high X-ray luminosities can be produced *only* as a result of star-disk magnetic reconnection phenomena. The example of YLW15, the only one so far for which we have evidence for superflares and periodic flaring, suggests that the underlying object must be a fast rotating star (i.e., near break-up) not yet magnetically locked to its accretion disk. In contrast, if this object is a slowly rotating star (i.e., far from break-up), its solar-like surface activity may be detected only in favourable circumstances, as in the case for WL6.

More generally, in addition to YLW15 and WL6, about a dozen protostars have been detected in X-rays so far, by ROSAT and/or by ASCA, with luminosities $L_X \gtrsim 10^{30-31} \text{ erg s}^{-1}$ (FM). Many, but not all, display X-ray flares, with time scales quite

comparable to those observed on T Tauri stars, possibly hotter ($T_X \sim$ a few keV) and more luminous. All are Class I and flat-spectrum protostars. However, the number of “X-ray loud” Class I protostars (including in ρ Oph EI29, IRS44 and IRS46) is only a few percent of their total number (Carkner et al. 1998). Sekimoto et al. (1997) have proposed that an orientation effect could be the reason, arguing that X-ray emitting protostars must be the ones seen pole-on because of the lower extinction along the funnel created in the envelope by molecular outflows. However, in the case of YLW15, the HST image clearly indicates that the accretion disk is viewed almost edge-on, and at least for this source an alternative interpretation is necessary.

In the context of the present paper, we can offer other reasons why the majority of Class I sources have not been detected yet in X-rays. First, reconnection phenomena may not necessarily occur on a regular basis, for instance because of various possible accretion instabilities, as discussed in the preceding subsection. (Recall that YLW15 itself was not detected during one previous ASCA observation.) Second, if its mass is low enough, the star may have already braked early in the Class I stage ($t_{br} < 10^5$ yrs) to reach corotation with the inner accretion disk. The very youngest may be X-ray bright, but in most cases only an underlying solar-like activity will go on, at levels lower than for WL6 for instance.

An intriguing property can also be explained in this context. To date, *all* the X-ray detected protostars belong to clusters (in addition to ρ Oph: RCrA, Chamaeleon, Orion), whereas none has been detected in Taurus, for example. We suggest that this is because clusters are the only place where stars can be found to be sufficiently massive ($M_* > 1 M_{\odot}$) to be fast rotators. Only lower-mass stars form in diffuse regions like Taurus, where the average stellar mass is more like $M_* \sim 0.5 M_{\odot}$: most protostars in such regions would presumably have reached magnetic locking by now, and therefore be the seat of an as yet undetectable low-level solar-like X-ray activity.

5.4. Areas of uncertainty

The preceding sections have shown that it is possible to construct a self-consistent model to explain the periodic X-ray flaring observed in the Class I protostar YLW15 by ASCA in terms of a reconnection within a magnetic loop sheared between a fast rotating star and a slowly rotating accretion disk. Thanks to this approach, it has been possible for the first time to recognize the fast-rotating status of a protostar, and propose an explanation for the existence of extremely luminous X-ray flares and other X-ray properties of protostars.

Now it must be realized that this construction rests on foundations that are not all certain, and more work is needed to confront them.

- The exact topology of magnetic field loops confining the X-ray emitting plasma during the decay phase is often subject to debate, since X-ray observations give access to the emission measure only ($EM = \int n_e^2 dV$), and examples are known (including on the Sun) of reheating phases during cooling. In the case of the triple flare of YLW15, however, the models with radiative cooling do not call for departures from a simple (if admittedly approximate) semi-circular magnetic loop. Thus, we consider the loop radius R_{loop} , which in our model plays an essential role to determine the beat period between the star and the disk, and thus *in fine* the stellar period, as reasonably well established. Data of better quality, such

as provided by the uninterrupted observations of *XMM* or *Chandra* will put more constraints on such models in the future.

- Although recent theoretical progress on MHD simulations of sheared magnetic configurations has been quite substantial, much remains to be done, especially in 3D, to even start comparing the results with “real” magnetic configurations resulting from star-disk shearing. We have used the numerical results obtained by Amari et al. (1996) for the time evolution of a twisted magnetic tube to infer that reconnection in the case of star-disk magnetic shearing should not occur much before one beat period, but of course actual calculations are required to validate this inference.
- The “classical” calculation of magnetic braking rests on the model initially proposed by Ghosh & Lamb (1978). This model assumes a steady-state solution to the problem of finding the balance between the star-disk magnetic torque and angular momentum variation. But as discussed above, at least in the case of fast rotation a steady-state situation likely does not hold; a possible manifestation is, precisely, magnetic shearing followed by reconnection and flaring on stellar rotation time scales. In addition, the interaction between the stellar magnetosphere and the inner disk remains poorly known, and the momentum loss mechanism is unclear. Our calculations of the corresponding braking time t_{br} are meant to represent the long-term evolution, and should still be taken as a rather rough approximation. Whether a collimated hot coronal wind actually contributes to the stellar angular momentum loss is also a possibility, but our calculations of the mass-loss rate (and of the inferred thermal radio emission) should be considered merely as a starting point. Nevertheless, the bottomline is that t_{br} seems to be of the same order as the duration of the Class I protostar phase, so that some of these protostars may still be rotating fast now, while others may have substantially spun down.
- The “mass-rotation” relation we have advocated, and in particular the limit between fast and slow rotators near the birthline, is correspondingly uncertain. Our calculations predict this limit should lie around $\approx 1 - 2M_{\odot}$, and existing observations tend to support this. However, too little is known observationally on the rotation of stars in this mass range and higher to be more conclusive: additional data must be obtained near the birthline, especially among the Herbig AeBe stars. The exact accretion geometry also plays a role and this is a concern as well.

Given these uncertainties, the present work may be considered as encouraging, but still exploratory.

6. SUMMARY AND CONCLUSIONS:

A TENTATIVE HISTORY OF PROTOSTELLAR ROTATION AND MAGNETIC ACTIVITY

We have studied the implications of an intense hard X-ray “triple flare” observed with *ASCA* at the level of $L_X \sim 10^{32}$ erg s^{-1} on the Class I protostar YLW15 in the ρ Oph cloud (analyzed in Paper I). With the reasonable assumption that magnetic shearing followed by reconnection between the central

star and the accretion disk is the basic heating mechanism for these flares, we find that the observed flare quasi-periodicity of ~ 20 h, probably also observed over 10 years ago by *Tenma*, is tracing the fast rotation of the central star. A key parameter in the demonstration is the size of the X-ray emitting region, which we model as a semi-circular magnetic loop of radius $\sim 4.5R_{\odot}$.

Given the evolved stage of Class I protostars, we further assume that the central star is on the “birthline” of the H-R diagram, so that a relation exists between its mass and its radius. Various constraints led us to the conclusion that the central star of YLW15 has $M_{\star} = 1.8 - 2.2M_{\odot}$ and $R_{\star} = 4.6 - 4.2R_{\odot}$, i.e., is a future A star. Another ρ Oph Class I protostar, WL6, more evolved than YLW15, and also detected by *ASCA*, displays an X-ray light curve which we interpret in terms of slow rotation, with a period ~ 3 days; its low bolometric luminosity places an upper limit to its mass of $M_{\star} \sim 0.4M_{\odot}$, and thus $R_{\star} \lesssim 2.7R_{\odot}$.

On the other hand, we have found that magnetic braking likely takes place on timescales of a few 10^5 yrs, i.e., *within the Class I stage*, so that both fast and slowly rotating protostars may coexist in the same star-forming region. These results obtained for YLW15 (fast rotation) and WL6 (slow rotation) support this finding, but are obviously subject to future confirmation (in particular from observations of other protostars with the upcoming generation of X-ray satellites). YLW15 and WL6 however belong the same star-forming region and are well documented at many wavelengths, which adds weight to the conclusions. We also found that *the main parameter for braking is the stellar mass*, since X-rays always indicate comparable values of the magnetic field (≈ 1 kG at the photospheric level). The accretion rate is also important, but a value of $\approx 10^{-6}M_{\odot} \text{ yr}^{-1}$ during the Class I protostar stage seems to be typical and fairly independent of the mass (for low- to intermediate-mass stars). With a duration of $\lesssim 2 \times 10^5$ yr for the Class I stage, we find that the boundary between fast and slow rotators at the birthline is $\approx 1 - 2M_{\odot}$.

More generally, since all the available X-ray evidence indicates that stellar rotation and magnetic activity are intimately related in low-mass stars, we may now put these results in a broader context. Moving backwards in time, we may propose the following scenario for the rotational evolution of protostars:

(i) At ages $\sim 10^5$ yrs, Class I protostars can be envisioned as Class II T Tauri stars embedded in a circumstellar envelope containing more mass when the star is younger. Their magnetic field, which may be primordial or dynamo-generated, exerts a braking torque on the accreting material in the vicinity of the central, growing star. Since the braking time is typically a \leq few 10^5 yrs, T Tauri-like synchronous rotation with the disk may be reached *during* the Class I stage, the exact moment depending on parameters like the mass (mainly) and the surface magnetic field and accretion rate and geometry (to a lesser extent). Young, fast rotating (and hence presumably more massive) Class I sources will be strong X-ray emitters due to star-disk interactions (YLW15), while evolved, less massive slow rotators will exhibit only solar-like X-ray activity near the surface of the central star (WL6). Fast-rotating Class I protostars may also be thermal radio emitters (from their hot coronal winds), and under very favourable circumstances, non-thermal radio emitters (from flaring activity).

(ii) At the early, build-up protostar stage (Class 0, ages $\lesssim 10^4$ yrs; see AWB), there is currently no observational indication of rotation: indeed, the fact that no Class 0 protostar has been

detected in X-rays so far can easily be attributed to their huge extinction (A_V up to ~ 1000) due to their massive envelope. Radio emission does not suffer from this drawback: the prototype Class 0 source, VLA1623, was first identified as a radio source. Thermal radio emission, one of the signatures of the Class 0 stage, may indirectly trace magnetic activity via a coronal wind, but as discussed in §2.4, it will probably not carry any rotation signature, contrary to the X-rays and possibly the non-thermal radio emission. Based on the Class I results presented in this paper, we can only speculate that the central object initially acquires angular momentum from its envelope and/or accretion disk, and builds up during the Class 0 phase in a state of fast, near break-up rotation. As is now well documented, outflows appear as soon as protostars exist (André, Ward-Thompson, & Barsony 1993; Bontemps et al. 1996). This can be due among others to an infall-ejection mechanism, guided by magnetic field lines (Henriksen & Valls-Gabaud 1994; Fiege & Henriksen 1996), or by a magnetocentrifugal mechanism reminiscent of the first version of the X-wind model proposed by Shu et al. (1988), which was based on break-up rotation of the central star. In such models, the magnetic field of the central object may be simply of interstellar origin and dragged during collapse. Reconections followed by coronal mass ejections or a

coronal wind may also play a role in launching YSO jets and/or outflows. Whatever the mechanism, it probably cannot be in a steady state if magnetic fields are important, in order to reconcile fast rotation and accretion.

The detection of X-rays from Class 0 protostars would of course be crucial in revealing their magnetic fields and estimating their strength, in tracing the rotation of the central, growing star, and in understanding the relations between accretion and outflow mechanisms. This will soon become possible up to $A_V \gtrsim 100$ with *XMM* owing to its high effective detection area. To clarify the relative importance of coronal and disk winds will require the help of sensitive very high-angular resolution radio interferometers. This class of observatories offer unprecedented opportunities to probe magnetic fields as an essential ingredient of star formation.

We thank Jean-Jacques Aly, Tahar Amari, Philippe André, Eric Feigelson, Kensuke Imanishi, Francesco Palla, Michel Tagger, and Yutaka Uchida for many useful discussions in the course of this work. We also thank an anonymous referee for stimulating remarks which helped to improve the clarity of the paper.

REFERENCES

- Adams, F.C., Lada, C.J., & Shu, F.H. 1987, *ApJ*, 312, 788
 Aly, J.-J. 1986, in *Magnetospheric Phenomena in Astrophysics* (New York: American Institute of Physics), p. 45
 Aly, J.-J., & Kuipers, J. 1990, *A&A*, 227, 473
 Amari, T., Luciani, J. F., Aly, J.-J., Tagger, M. 1996, *ApJ*, 466, L39
 André, P. 1987, in *Protostars and Molecular Clouds*, Eds. T. Montmerle & C. Bertout (Saclay: Doc. CEA), p. 143
 André, P., Deeney, B. D., Phillips, R. B., Lestrade, J.-F. 1992, *ApJ*, 401, 667
 André, P., & Montmerle, T. 1994, *ApJ*, 420, 837
 André, P., Ward-Thompson, & Barsony, M. 1993, *ApJ*, 406, 122
 André, P., Ward-Thompson, & Barsony, M. 2000, in *Protostars & Planets IV*, Eds. V. Mannings, A. Boss, & S. Russell (Tucson: U. Arizona Press), *in press* (AWB)
 Babel, J., & Montmerle, T. 1997, *ApJ*, 485, L29
 Barsony, M., Kenyon, S. J., Lada, E.A., & Teuben, P.J. 1997, *ApJ Suppl.*, 112, 109
 Bell, K. R., Cassen, P. M., Klahr, H. H. & Henning, T. 1997, *ApJ*, 486, 372
 Bertout, C., Basri, G., & Bouvier J. 1988, *ApJ*, 330, 350
 Birk, G. T. 1998, *A&A*, 330, 1070
 Boehm, T., & Catala, C. 1995, *A&A*, 301, 155
 Bontemps, S., André, P., Terebey, S., & Cabrit, S. 1996, *A&A*, 311, 858
 Bouvier, J. 1990, *AJ*, 99, 946
 Bouvier, J., et al. 1999, *A&A*, 349, 619
 Camenzind, M. 1997, in *Herbig-Haro Flows and the Birth of Low Mass Stars*, Eds. B. Reipurth & C. Bertout (Dordrecht: Kluwer), p. 241
 Carkner, L., Kozak, J. A., & Feigelson, E. D. 1998, *AJ*, 116, 1933
 Casanova, S. 1994, PhD Thesis, Université Paris VI
 Chiang, E.I., & Goldreich, P. 1999, *ApJ*, 519, 279
 Dame, T. M., et al. 1987, *ApJ*, 322, 706
 Edwards, S., Hartigan, P., Ghandour, L. & Andrulis, C. 1994, *AJ*, 108, 1056
 Feigelson, E.D., Carkner, L., & Wilking, B.A. 1998, *ApJ*, 494, L215
 Feigelson, E.D., & Montmerle, T. 1999, *ARA&A*, 37, 363 (FM)
 Fendt, C., & Elstner, D. 1999, *A&A*, 349, L61
 Fiege, J.D., & Henriksen R.N. 1996, *MNRAS*, 281, 1038
 Ghosh, P. & Lamb, F. K. 1978, *ApJ*, 223, L83
 Ghosh, P. & Lamb, F. K. 1979, *ApJ*, 234, 296
 Glassgold, A.E., Najita, J., & Igea, J. 1997, *ApJ*, 480, 344 (Erratum in *ApJ*, 485, 920)
 Glassgold, A.E., Feigelson, E.D., & Montmerle, T. 2000, in *Protostars & Planets IV*, Eds. V. Mannings, A. Boss, & S. Russell (Tucson: U. Arizona Press), *in press*
 Goodson, A. P., Winglee, R. M., & Boehm, K. -H. 1997, *ApJ*, 489, 199
 Grosso, N., Montmerle, T., Feigelson, E.D., André, P., Casanova, S., & Gregorio-Hetem, J. 1997, *Nature*, 387, 56
 Hartmann, L., Kenyon, S., & Hartigan, P. 1993, in *Protostars & Planets III*, Eds. E.H. Levy & J. Lunine (Tucson: U. Arizona Press), p. 497
 Hayashi, M. R., Shibata, K. & Matsumoto, R. 1996, *ApJ*, 468, L37
 Hayashi, M., Shibata, K., & Matsumoto, R. 1998, *IAU Symposia*, 188, 232
 Henriksen, R.N., André, P., & Bontemps, S. 1997, *A&A*, 323, 549
 Henriksen, R.N., & Valls-Gabaud, D. 1994, *MNRAS*, 266, 681
 Hirose, S., Uchida, Y., Shibata, K., & Matsumoto, R. 1997, *PASJ*, 49, 193
 Innes, D. E., Inhester, B., Axford, W. I. & Wilhelm, K. 1997, *Nature*, 386, 811
 Johns-Krull, C.M., Valenti, J.A., Koresko, C. 1999, *ApJ*, 516, 900
 Kamata, Y., Koyama, K., Tsuboi, Y., & Yamauchi, S. 1997, *PASJ*, 49, 461
 Kenyon, S. J. & Hartmann, L. 1987, *ApJ*, 323, 714
 Koyama, K. 1987, *PASJ*, 39, 245
 Koyama, K., Hamaguchi, K., Ueno, S., Kobayashi, N. & Feigelson, E. D. 1996, *PASJ*, 48, L87-L92
 Koyama, K., Maeda, Y., Ozaki, M., Ueno, S., Kamata, Y., Tawara, Y., Skinner, S., & Yamauchi, S. 1994, *PASJ*, 46, L125
 Königl, A. 1991, *ApJ*, 370, L39
 Königl, A., & Pudritz R.E. 2000, in *Protostars & Planets IV*, Eds. V. Mannings, A. Boss, & S. Russell (Tucson: U. Arizona Press), *in press*
 Lada, C. J., & Wilking, B. A. 1984, *ApJ*, 287, 610
 Leous, J.A., Feigelson, E.D., André, P., & Montmerle, T. 1991, *ApJ*, 379, 683
 Lovelace, R. V. E., Romanova, M. M., & Bisnovatyi-Kogan, G. S. 1995, *MNRAS*, 275, 244
 Luhman, K.L., & Rieke, G.H. 1999, *ApJ*, *in press*
 Miller, K. A., & Stone, J. M. 1997, *ApJ*, 489, 890
 Montmerle, T., Koch-Miramond, L., Falgarone, E., & Grindlay, J.E. 1983, *ApJ*, 269, 182
 Motte, F., André, P., & Neri, R. 1998, *A&A*, 336, 150 (MAN)
 Muzerolle, J., Hartmann, L., & Calvet, N. 1998, *AJ*, 116, 455
 Oster, L. 1961, *Rev. Mod. Phys.*, 33, 525
 Palla, F., & Stahler, S. W. 1992, *ApJ*, 392, 667
 Palla, F., & Stahler, S. W. 1993, *ApJ*, 418, 414 (PS)
 Reynolds, S. 1986, *ApJ*, 304, 713
 Rodríguez, L.F. 1997, in *Herbig-Haro Flows and the Birth of Low Mass Stars*, Eds. B. Reipurth & C. Bertout (Dordrecht: Kluwer), p. 83
 Sekimoto, Y., Tatsumatsu, K., Umamoto, T., Koyama, K., Tsuboi, Y., & Hirano, N. 1997, *ApJ*, 489, L63
 Shu, F. H. 2000, in *Protostars & Planets IV*, Eds. V. Mannings, A. Boss, & S. Russell (Tucson: U. Arizona Press), *in press*
 Shu, F. H., Adams, F.C., & Lizano, S. 1987, *ARA&A*, 25, 23
 Shu, F. H., Lizano, S., Ruden, S. P., & Najita, J. 1988, *ApJ*, 328, L19
 Shu, F. H., Shang, H., Glassgold, A. E., & Lee, T. 1997, *Science*, 277, 1475
 Skinner, S. L., Güdel, M., Koyama, K., & Yamauchi, S. 1997, *ApJ*, 486, 886
 Stahler, S.W. 1988, *ApJ*, 332, 804
 Stelzer, B., Neuhauser, R., Casanova, S., & Montmerle, T. 1999, *A&A*, 344, 154
 Tagger, M., & Pellat, R. 1999, *A&A*, *in press*
 Terebey, S., Shu, F. H. & Cassen, P. 1984, *ApJ*, 286, 529
 Tsuboi, Y., Imanishi, K., Koyama, K., Grosso, N., & Montmerle, T. 1999, *ApJ*, *in press* (Paper I)
 Van den Oord, G.H.J. & Mewe, R. 1989, *A&A*, 213, 245
 Wang, Y.-M. 1996, *ApJ*, 465, L111
 Wilking, B. A., & Lada, C. J. 1983, *ApJ*, 274, 698
 Wilking, B.A., Lada, C.J., & Young, E.T. 1989, *ApJ*, 340, 823
 Young, E. T., Lada, C. J., & Wilking, B. A. 1986, *ApJ*, 304, L45